NASA-TM-111194

Pergamon

0892-9270(93)E0007-Y

Space Technol. Vol. 14, No. 1, pp. 31–44, 1994
Elsevier Science Ltd. Printed in Great Britain

LOW THRUST CHEMICAL ROCKET TECHNOLOGY*

STEVEN J. SCHNEIDER
NASA Lewis Research Center, Cleveland, OH 44135, U.S.A.

Abstract—An on-going technology program to improve the performance of low thrust chemical rockets for spacecraft on-board propulsion applications is reviewed. Improved performance and lifetime is sought by the development of new predictive tools to understand the combustion and flow physics, introduction of high temperature materials and improved component designs to optimize performance, and use of higher performance propellants. Improved predictive technology is sought through the comparison of both local and global predictions with experimental data. Predictions are based on both the RPLUS Navier–Stokes code with finite rate kinetics and the JANNAF methodology. Data were obtained with laser-based diagnostics along with global performance measurements. Results indicate that the modeling of the injector and the combustion process needs improvement in these codes and flow visualization with a technique such as two-dimensional laser-induced fluorescence (LIF) would aid in resolving issues of flow symmetry and shear layer combustion processes. High temperature material fabrication processes are under development and small rockets are being designed, fabricated, and tested using these new materials. Rhenium coated with iridium for oxidation protection was produced by the Chemical Vapor Deposition (CVD) process and enabled an 800 K increase in rocket operating temperature. Performance gains with this material in rockets using Earth storable propellants (nitrogen tetroxide and monomethylhydrazine or hydrazine) were obtained through component redesign to eliminate fuel film cooling and its associated combustion inefficiency while managing head end thermal soakback. Material interdiffusion and oxidation characteristics indicated that the requisite lifetimes of tens of hours were available for thruster applications. Rockets were designed, fabricated, and tested with thrusts of 22, 62, 440 and 550 N. Performance improvements of 10 to 20 seconds specific impulse were demonstrated. Higher performance propellants were evaluated. These propellants, defined as space storable propellants, include liquid oxygen (LOX) as the oxidizer with nitrogen hydrides or hydrocarbons as the fuels. Specifically, a LOX/hydrazine engine was designed, fabricated, and demonstrated to have a 95% theoretical c-star which translates into a projected vacuum specific impulse of 345 s at an area ratio of 204:1. Further performance improvement can be obtained by the use of LOX/hydrogen propellants, especially for manned spacecraft applications, and specific designs must be developed and advanced through flight qualification.

INTRODUCTION

Currently, a NASA-OAET supported technology program is underway to provide improved performance low thrust chemical rockets for on-board propulsion. The state-of-the-art consists of rockets employing Earth storable propellants (nitrogen tetroxide and monomethylhydrazine or hydrazine) in radiation cooled thrust chambers fabricated from niobium (C-103) with a fused silica coating (R512A or R512E) for oxidation protection. This technology for these relatively long-life applications is over 20 years old. On-board propulsion applications include reaction control of launch vehicles, attitude control and positioning of low Earth orbit satellites, apogee insertion and north–south station keeping of geosynchronous satellites, and "delta-V" and retropropulsion of planetary spacecraft. The program includes contract, grant, and in-house activities in the areas of predictive technology, system analysis, and component development.

This paper reviews the recent progress in this broad technology program. Efforts to understand the fundamental physical and chemical processes occurring in small rockets by comparisons of both local laser-based diagnostic data and global performance data with predictive technologies are discussed first. Then, the technology program to understand the life-limiting phenomena occurring in new high-temperature materials for the thrust chamber is discussed, followed by the program to introduce new materials to operational use. Finally, the system analyses and technical efforts aimed at developing a technology base for higher performance propellants are presented. Technology transfer to useful applications is the primary goal of the program.

PREDICTIVE TECHNOLOGY

Performance prediction of rocket engines, in general, is commonly achieved with the Joint Army, Navy, NASA, Air Force (JANNAF) Two-Dimensional Kinetics code with a boundary layer module (TDK/BLM) [1] and empirical injector-combustion chamber performance data. An inviscid, axisymmet-

*Paper IAF-92-0669 presented at the *43rd Congress of the International Astronautical Federation*, Washington, D.C., 28 August–5 September 1992.

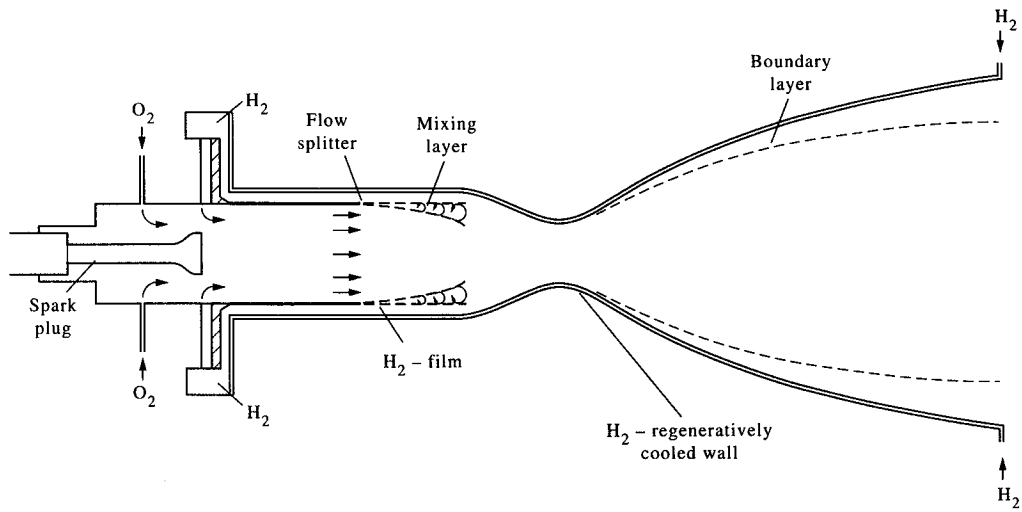

Fig. 1. Schematic of flowfield in 110 N thruster used for diagnostics and model comparisons.

ric flowfield is calculated by the method of characteristics from which boundary layer, kinetics, and other losses are subtracted. This methodology is very useful for small rockets, but has in general led to the overprediction of their performance [2]. The flow fields of small rockets differ from those of medium to launch class rockets in that the boundary layers and associated losses in small rockets are proportionally larger. Injectors in small rockets are more difficult to model by zonal analysis, and mixing efficiency and heat transfer rates in the presence of fuel film cooling are largely unknown.

Navier–Stokes analyses

In-house [3] and grant [4, 5] activities are underway to solve the full Navier–Stokes equations with finite rate kinetics in the converging-diverging nozzle geometry of a small rocket. An existing computer code named RPLUS [6] was selected and modified for axisymmetric flow to calculate thruster flowfields. This code was selected because of its ability to couple finite rate kinetics into the Navier–Stokes solution, a phenomenon important to low chamber pressure rockets. One calculation [7] of a higher thrust rocket (2200 N), with a 1030:1 area ratio nozzle, demonstrated the viability of the RPLUS code for calculations of large area ratio nozzle flows. The Van Driest's damping constant in the inner-layer model of the Baldwin–Lomax turbulence model was modified to successfully predict relaminarization of the turbulent boundary layer due to the favorable pressure gradient.

Hydrogen/oxygen flowfields were calculated on the 110 N thruster geometry, shown in Fig. 1, where the calculation began at the trailing edge of the flow splitter. For lack of a more accurate description, these calculations assumed uniform equilibrium inflow boundary conditions and adiabatic walls. Slow convergence in the subsonic flow was characteristic of the calculation. Measured performance trends with mixture ratio and percent fuel film cooling were accurately predicted, but, as shown in Fig. 2, measured performance values were underpredicted [4, 8] by 3–4%. Both the inflow boundary condition and adiabatic wall have the effect of increasing calculated performance values and cannot account for this discrepancy. The low predictions of performance in this case may indicate inaccurate modeling of the core flow/film flow mixing. Turbulence modeling was suspected, but both the k-ϵ [4] and Baldwin–Lomax model modified with Prandtl's mixing length model [3, 8] gave similar results. The Reynolds numbers, however, were low enough for this geometry that there was some question as to whether the flow was laminar or turbulent. If laminar, the shear layer could contain large scale, orderly structures transporting mass across the shear layer. Possible contributions to the shear layer mixing by three-dimensional effects at

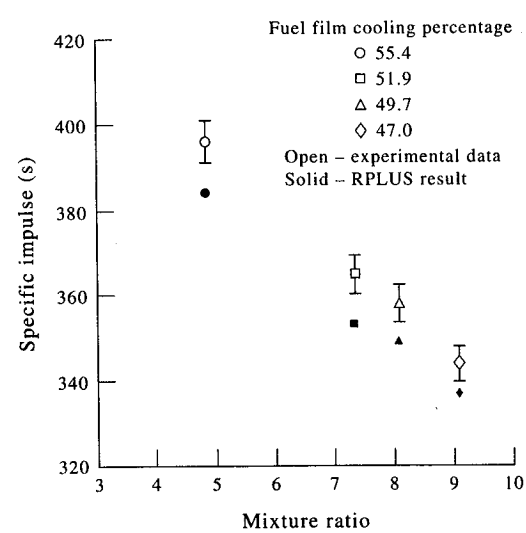

Fig. 2. Underprediction of global performance by 3–4% by Navier–Stokes model [8].

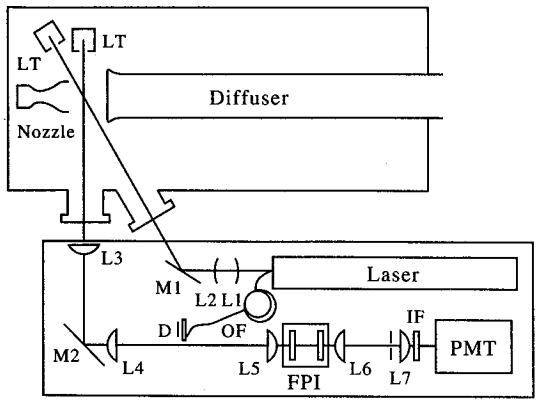

Fig. 3. Schematic of Rayleigh optical configuration used for rocket plume measurements [11].

the point of hydrogen film injection were evaluated experimentally using an axisymmetric and finned sleeve insert [9]. These geometry changes were found to influence performance only within experimental error (except for one case) and, hence, were not the source of any enhanced mixing.

Comparisons of data and analyses

A new in-house low thrust chemical rocket test facility [10] was used for experimental comparisons with predictions and for rocket component evaluation. The facility currently has gaseous hydrogen/oxygen propellant capability and is capable of maintaining altitude up to 37 km. This enabled tests of 110 N class rockets with chamber pressures of 690 kPa and nozzles with 30:1 area ratio. The facility is currently being upgraded to include liquid oxygen/hydrocarbon test capabilities for the space storables technology discussed later in this paper. Recent tests conducted in the facility included long duration rocket chamber material tests and classical performance evaluations of injectors, ignitors, and nozzles.

A suite of laser-based diagnostics, including Rayleigh and Raman spectroscopy, were installed in support of the predictive technologies. The Rayleigh diagnostic [11] was spectrally resolved and was used for rocket plume studies near the exit plane of 30:1 area ratio nozzle. The capability to measure gas temperature, density, and velocity in a hydrogen–oxygen plume (predominantly water vapor) was demonstrated by resolving the spectrum of molecularly scattered light from an argon–ion laser with a scanning Fabry–Perot interferometer. A schematic of the optical configuration used in the rocket test cell is shown in Fig. 3. The flow was practically free of particulate and the problem of stray laser light was successfully handled with light traps, baffles, and carefully placed apertures. This is critical for the Rayleigh diagnostic since the scattered light is essentially at the laser frequency. The amount of stray light collected significantly altered the spectrum measured by the photon counter, as shown in Fig. 4, which shows Rayleigh spectra taken on two different days at the same point in the nozzle flow. One had a high level of wall scatter and the other a low level. This difference in the measured spectra was successfully taken into account by the spectral model function used to curve fit the data, as shown by the solid lines in Fig. 4. The parameter estimates for temperature, density, and velocity were almost equal for the two spectra shown (i.e. 1100 K, $5.0 \times 10^{22}/m^3$, 4200 m/s).

The rocket plume flowfield of a 110 N thrust, 730 kPa chamber pressure, 30:1 area ratio nozzle, gaseous hydrogen/gaseous oxygen rocket operating at an overall mixture ratio of 6.7 with 15% fuel film-cooling was measured using this Rayleigh diagnostic and compared with both the JANNAF and Navier–Stokes (RPLUS) predictions [12]. Both predictive models were extended into the plume region for direct comparison with the data. TDK [1] was extended by the use of the Standardized Plume Flowfield (SPF) [13] code. The TDK prediction was for a single zone flow at a mixture ratio of 6.7 and chamber pressure of 730 kPa. A uniform inflow boundary condition with 100% combustion efficiency was assumed in the prediction. The RPLUS prediction assumed a two zone inflow boundary condition

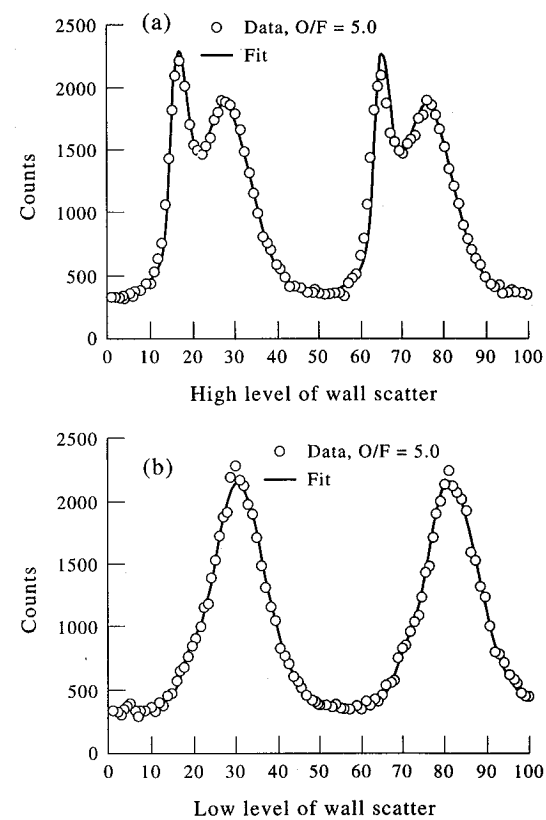

Fig. 4. Spectrally resolved Rayleigh light with high and low levels of wall scatter at the same point in the flow. Spectral model function gives the same parameter estimate for both spectra [11].

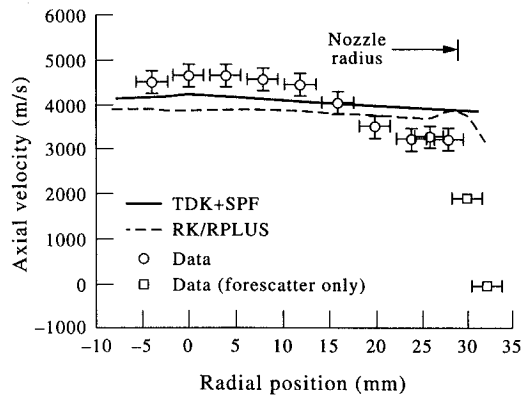

Fig. 5. Axial velocity measurement in a rocket plume via Rayleigh spectroscopy and comparison with predictive models [12].

with a core flow mixture ratio of 8.0 and 15% fuel film-cooling to achieve the overall mixture ratio of 6.8. The experimental mass flow rate was an input in the calculation. The axial velocity and static temperature profile comparisons are shown in Figs 5 and 6, respectively. Velocity data were resolved into axial and radial components of velocity with a forescatter and backscatter optical arrangement where the forescatter measured predominantly axial velocity. In Fig. 5, note the very flat velocity profiles predicted by both TDK and RPLUS in contrast to the nearly parabolic velocity profile which was measured. This was believed to be due to inaccurate modeling of the injector, which was assumed to provide uniform inflow conditions to both predictions. Note also the unexplained plateau in velocity between radial positions 24 and 28 mm. The determination was not made as to whether this is due to fuel film-cooling or injector streaking. If it was the former, the RPLUS code failed to model the film-core interaction accurately because an increase in film velocity was predicted between radial positions 28 and 30 mm. The measured temperature profile in Fig. 6 fell below both predictions, except for the centerline TDK prediction.

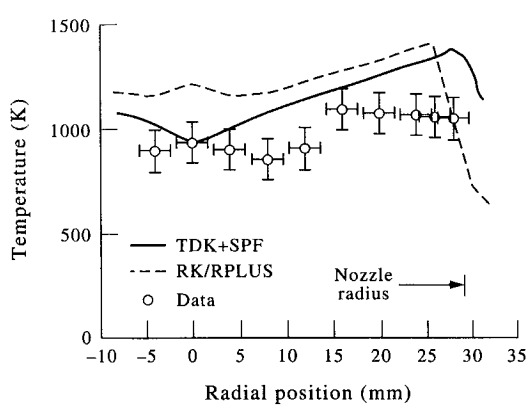

Fig. 6. Temperature measurement in a rocket plume via Rayleigh spectroscopy and comparison with predictive models [12].

Higher measured velocities inside the 15 mm radius could lower the measured static temperature and account, in part, for this disagreement. Outside the 15 mm radius, unsteady transition flow could account for a larger transport scale for film-core mixing than was predicted by the turbulence model or streaking could also result in the lower temperature data. This was consistent with the sharp drop in the RPLUS predicted static temperature outside the radial position of 26 mm, which implied a smaller transport scale for mixing between the core and film than was shown in the data. (The temperature offset between TDK and RPLUS was due to the core inflow boundary temperatures which are based on the measured overall mixture ratio of 6.7 and measured chamber pressure of 730 kPa for TDK and the estimated core mixture ratio of 8.0 and measured mass flow of 0.033 kg/s which yielded a chamber pressure of 841 kPa for RPLUS.) The complete set of Rayleigh measurements of density, velocity, and temperature, when assumed axisymmetric and integrated over the exit plane, enabled a comparison with globally measured thrust and mass flow. The thrust and mass flow estimates from the Rayleigh data were within 2% of the measured values, which provided confidence in the local Rayleigh measurements.

The Raman diagnostic was installed with optical fiber transmission of both the high power probe beam to the rocket plume and the Raman signal to the spectrometer [14]. This diagnostic was also spectrally resolved and a schematic of the facility is shown in Fig. 7. Data are shown in Fig. 8 of a spectral scan of the oxygen Q-branch for a point in both ambient air and the plume of a hydrogen/oxygen rocket with a 1.85:1 area ratio nozzle [15]. Calibration factors were obtained by curve fitting a theoretical spectrum, as shown, to the known oxygen concentration in the ambient air and then curve fitting the spectrum from the rocket. Oxygen number density and temperature were derived from the curve fit.

Raman data were obtained in the rocket plume flowfield of a 110 N thrust, 453 kPa chamber pressure, 1.85:1 area ratio nozzle of a gaseous hydrogen/gaseous oxygen rocket operating at an overall mixture ratio of 5.13 with 75% fuel film-cooling. The oxygen number density and temperature are given in Figs 9 and 10, respectively, and were compared with a prediction by the RPLUS code. The RPLUS model again assumed a two zone inflow boundary condition with uniform flow in each zone. Equilibrium conditions, at a mixture ratio of 20, were specified as the inflow boundary condition for the core. The measurements were obtained along a radius in a plane 10 mm downstream of the nozzle exit plane and, for the most part, fall between an exit plane prediction ($Z = 0$) and a measurement plane prediction ($Z = 10$ mm) by RPLUS. Effects of facility backpressure and combustion inefficiency were not incorporated into the RPLUS model and were likely contributors to the discrepancy between data and theory. The prediction

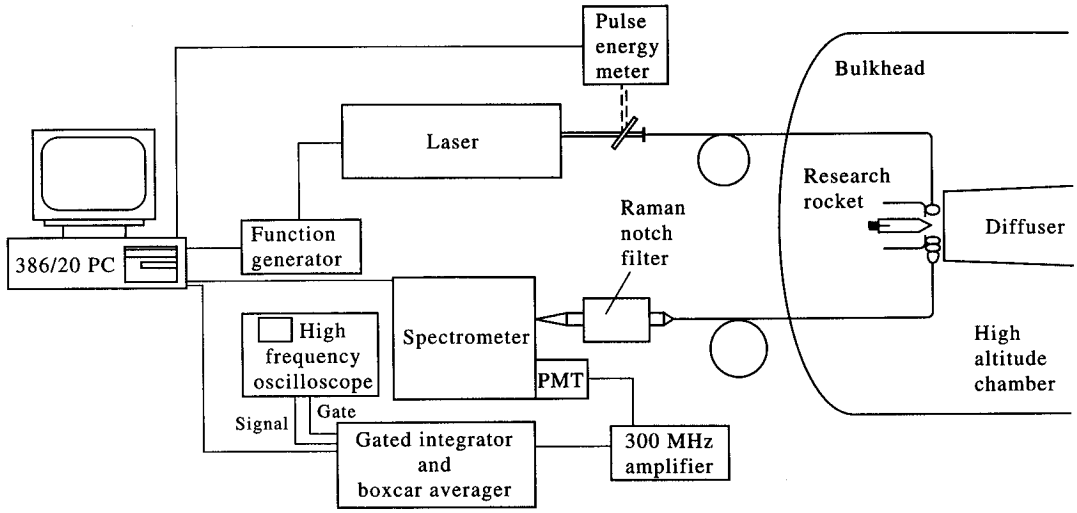

Fig. 7. Schematic of Raman diagnostic used for rocket plume measurements showing optical fiber transmission of both probe and signal beams [14].

was one of an underexpanded flow expanding into a vacuum while the measurements were taken in underexpanded flow expanding to a backpressure between 2 and 6 kPa. This could account for the smaller than predicted radial extent of O_2. This collapse of the plume along with combustion inefficiency could contribute to the high measured O_2 number density near the centerline. A core flow combustion efficiency of 100% was assumed at the inlet boundary in the RPLUS model leading to low predicted O_2 concentrations in this oxidizer rich flow. The experimentally measured temperature profile in Fig. 10, was 10–15% higher than the predicted temperature at $Z = 10$ mm. The measured local maximum in temperature at a radial position off the centerline was believed to result from the combusting shear layer between the oxidizer rich core and the fuel film-cooling. While the agreement between temperature data and theory is reasonable, a contributor to the discrepancy could be a larger experimental transport scale between the film and core flows, resulting in more shear layer combustion and higher temperatures. Measurements using the O_2 molecule could not be taken beyond the radius of 7.5 mm due to low oxygen concentration, so facility effects on the radial extent of the plume, believed to be rich in H_2, were not determined.

Based on the comparisons of predictions with local and global rocket measurements to date, it is felt that the shear layer combustion model in the predictions needs improvement, possibly incorporating transport phenomena existing in transition flows, and that the computational domain should be extended into the near injector flow. The latter effort requires computational schemes with more rapid convergence in the subsonic flow and probably requires 3-D modeling of the gaseous propellant injection. The diagnostic suite

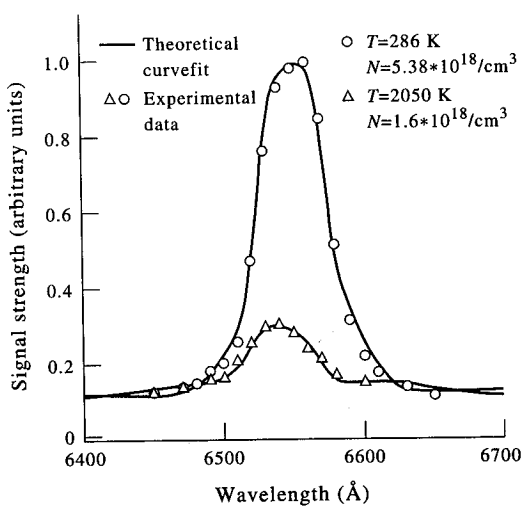

Fig. 8. Spectrally resolved Raman Q-branch for oxygen with theoretical parameter curvefit [14].

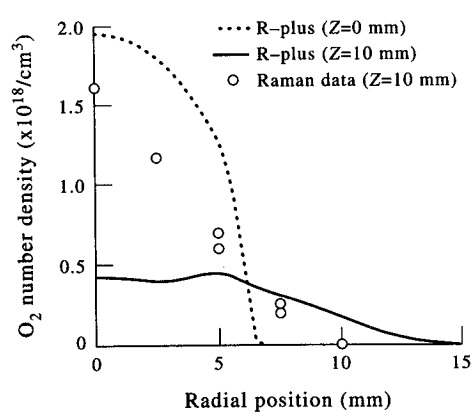

Fig. 9. Oxygen number density measured by Raman spectroscopy in a rocket plume and comparison with predictive model [14].

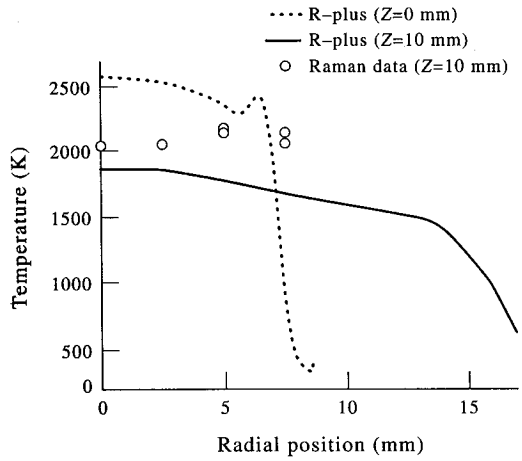

Fig. 10. Plume temperature measured by Raman spectroscopy and comparison with predictive model [14].

is being expanded to include Laser-Induced Fluorescence (LIF). Two-dimensional LIF images of the flow will be used to resolve issues of flow symmetry in the analyses and to visualize the shear layer mixing process in an optically accessible thruster. Additional Rayleigh and Raman data will be obtained on different injectors, chambers, and nozzles to determine the effects of rocket design parameters on measured flowfields and for comparison with the modeling effort.

Spray combustion modeling

A modeling effort was also conducted for liquid bipropellant spary combustion and flow modeling in small rocket engines [16]. This effort involved phenomena that are much more complex than those in gaseous propellant rockets in that liquid propellant spray dynamics and heterogeneous chemical reactions, as well as homogeneous reactions and turbulent gas transport, were incorporated into the model. A predictive tool for liquid bipropellant rocket combustors was assembled within the computational framework of KIVA-II [17] combustion code for gas turbine combustors. The model encompassed a computational technique for the gas-phase governing equations, bipropellant spray injection as discrete particles, and constitutive models for combustion chemistry and interphase exchanges, i.e. gas phase chemistry, droplet vaporization, propellant impingement (both hypergolic and nonhypergolic), and droplet breakup/coalescence. Applications to demonstrate the capabilities of the code were calculated [18]. The chosen chamber geometry was that of a single element pintle injector with an unlike doublet injection allowing an axisymmetric model. Two different propellant combinations, i.e. N_2H_4/N_2O_4 and N_2H_4/LOX, were calculated. Efforts to establish the usefulness of this code are on-going with experimental data from the space storable technology program using N_2H_4/LOX propellants.

HIGH TEMPERATURE MATERIALS

A program to improve the performance of small radiation-cooled thrusters by increasing their operating temperature with new materials is underway. Improved performance was obtained by reducing or eliminating fuel film-cooling in rocket combustors, resulting in increased combustion efficiency and lower plume contamination from unburned propellants.

Background

Nearly every film and radiation cooled liquid rocket thrust chamber and exit nozzle presently is fabricated from niobium (C-103) with a fused silica coating (R-512A or R-512E) for oxidation protection. The life of the coating is limited by two modes of degradation. The first and most understood mode is the loss of the coating due to diffusion and vaporization of the material. This mode can be evaluated by available analytical techniques based on diffusion and vapor pressure relationships. The second mode of degradation is the result of differences in the coefficient of thermal expansion of the C-103 base material and the R-512 coating. The repeated cycling of the material system between room temperature and elevated temperature (1400–1900 K) results in coating cracking and eventual spalling. In addition, the cracks formed result in substrate oxidation and this can result in additional spalling of the coating and eventual exposure of the C-103 to the combustion gases.

No definitive analytical technique has been found which can predict the onset of coating failure based on a combination of "time at elevated temperature" and number of thermal cycles. The recommended life limits (time at elevated temperature) used by several rocket manufacturers is given in Fig. 11. These data were based on torch tests of materials and qualification tests of rocket engines conducted by these companies. Note a significant variability in recommended life, but a general agreement that there is 10–15 h of

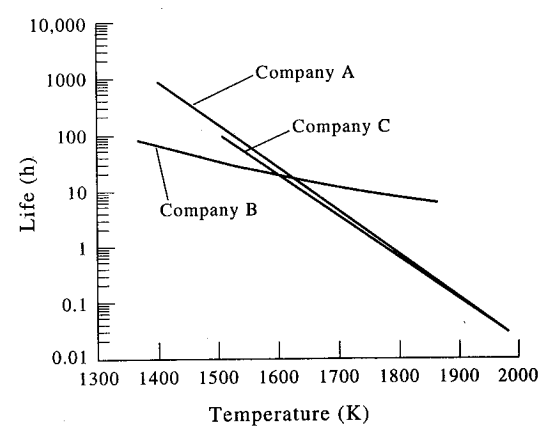

Fig. 11. Recommended life limits of silicide coated Nb used by several rocket manufacturers.

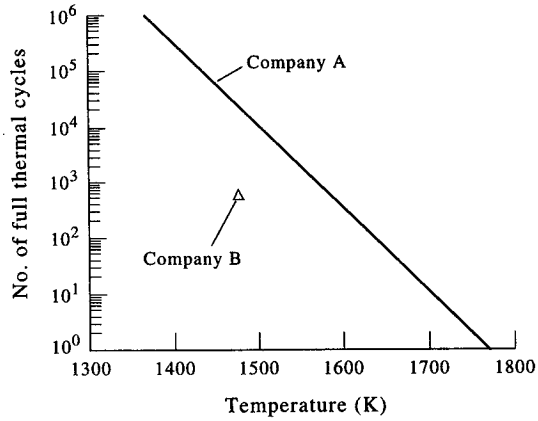

Fig. 12. Recommended number of full thermal cycles vs peak cycle temperature for silicide coated Nb used by rocket manufacturers.

life at around 1640 K. One manufacturer also reports that life may be dependent on thruster size.

For cyclic applications, manufacturer recommended life limits are expressed as the number of full thermal cycles versus peak cycle temperature, as given in Fig. 12. These data indicate that for high engine temperature, this coating cannot withstand many (100–1000) thermal cycles without failing. For mixed steady state and pulse duty operation, manufacturers recommend addition of the steady state and cyclic components of life. For example, using the most conservative data from Figs 11 and 12, a thruster life is defined as steady state operation for 6 h (50% of life) plus pulse duty operation for 300 cycles (50% of life) at 1470 K.

Iridium-coated rhenium

Rhenium coated with iridium for oxidation protection was the first thrust chamber material chosen for development under this program [19, 20]. This selection was made following a literature and vendor survey of potential materials with capabilities of operating at temperatures as high as 2470 K in an oxidizing rocket engine environment.

Refractory metals, ceramics, composites, and carbon–carbon materials were evaluated for substrate materials. Platinum group metals, Engle–Brewer compounds and ceramics were considered for oxidation resistant coatings. Iridium–rhodium–rhenium alloys and ceramic/metal (CERMET) alloys were considered as monolithic materials. Many candidate materials were available, but most had very little information available about their fundamental properties of interest such as strength, shock resistance, and oxidation resistance. In addition, some very promising materials required extensive development of their fabrication technologies.

Rhenium (Re) was selected as the substrate material because of its high melting point (3400 K), excellent strength at high temperature, and absence of a ductile-to-brittle transition common in other refractory metals. Iridium (Ir) was chosen as the oxidation resistant coating for rhenium because of its adequate melting temperature (2720 K), good oxidation resistance (3 orders of magnitude better than Re), close coefficient of thermal expansion to rhenium, adherence to rhenium, and ductility.

These materials were first fabricated for the Air Force Rocket Propulsion Laboratory [21, 22] in the form of 3 mm diameter tubes by the Chemical Vapor Deposition (CVD) technique. Oxidation tests were performed by induction heating of the samples in air to 2270 K for over 20 min. The iridium coating, however, was porous and did not afford the requisite oxidation protection to the underlying rhenium. Further development [23] of the iridium CVD process yielded uniform, non-porous coatings that offered excellent oxidation protection to the rhenium. Small 22 N rocket chambers were fabricated to evaluate this material. They were mated to a water cooled injector and fired with nitrogen tetroxide/monomethylhydrazine (N_2O_4/MMH) propellants as a material demonstrator. Over 15 h [19, 24] of operation and 2684 thermal cycles at temperatures around 2500 K were demonstrated without failure. A summary of test time vs mixture ratio is given in Table 1. Following these tests, the measured throat diameter had increased only about 0.01 mm and the chamber weight loss was less than 1%.

In order to understand the performance limits of Ir-coated Re thrusters, an effort [20, 25] is underway at the Sandia Combustion Research Facility to measure interdiffusion and oxidation kinetics of Ir-coated Re. Gas phase measurements were obtained near the surface of heated samples in an atmospheric pressure air/H_2 flame by laser-induced fluorescence [25, 26]. Hydroxyl radical (OH) measurements significantly above equilibrium were measured for almost all test conditions and no differences in profiles near iridium or platinum samples were observed. This suggested that the OH concentrations near the surface were determined primarily by a radical recombination process in the post-flame gases, or else these

Table 1. 22 N iridium coated rhenium material demonstrator rocket test summary [19]

MR	Maximum temperature (K)	No. of thermal cycles	Duration (s)
1.45		2	61
1.50		3	70
1.55	—	2	10
1.60	—	2	2705
1.65	2478	581	31457
1.70	2511	571	15856
1.75	—	1	2
1.80	2496	503	2210
1.85	—	2	10
1.90	2513	551	1105
2.00	2519	366	738
2.05	2519	100	200
Totals		2684	54430

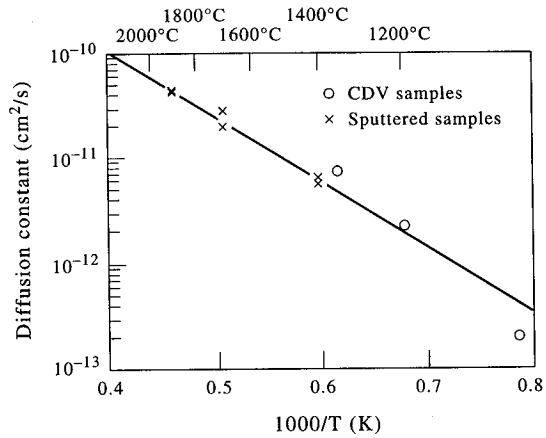

Fig. 13. Measured diffusion constants of iridium-rhenium couples showing Arrhenius dependence [28].

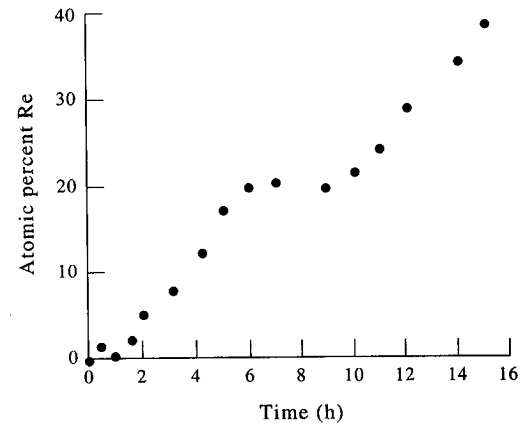

Fig. 14. Bulk concentration of rhenium in the near surface of iridium as a function of time during 2373 K anneal in ultrahigh vacuum [29].

surfaces have the same reactivities. The oxidation kinetics of Ir remain, however, to be determined.

Surface reaction phenomena on samples heated in a furnace were examined using Raman spectroscopy, Auger spectroscopy and X-ray diffraction [25, 27, 28]. Analysis of samples showed that Ir was attacked and etched by oxygen through the formation and desorption of IrO_2. An Ir recession rate of 0.15 μm/h was measured [19] by thermogravimetric analysis (TGA) at 1810 K in Ar + 0.5% O_2 at 190 Pa. Ir–Re interdiffusion was examined by annealing Ir-coated Re samples in a vacuum furnace at temperatures between 1670 and 2370 K. The samples were cross-sectioned and polished and electron microprobe analysis was used to determine the distribution of Re and Ir in these annealed coatings. Re was observed to diffuse preferentially along grain boundaries into the Ir coating with very little diffusion of Ir into the Re. Diffusion constants were obtained by a model of diffusion into a semi-infinite medium where the boundary was held at constant concentration. Measured diffusion constants are given in Fig. 13. They have an Arrhenius dependence with an activation energy for diffusion of 1.23 eV. This activation energy was well below that expected for bulk diffusion, which suggested that grain boundary diffusion was the dominant diffusion mechanism and implied that the large iridium grains produced by CVD were desirable for the low diffusion rates.

In another test, rhenium concentration at the iridium surface was monitored with an Auger spectrometer, while the sample was resistively heated to 2370 K in an ultrahigh vacuum for 15 h [29]. The results are shown in Fig. 14. Note that the Re concentration appeared to saturate at about 20 at.% in iridium, but eventually rose further. This was believed to correspond to the solubility limit for Re in Ir, which is nominally around 30% (but not well determined). This result could have a favorable impact on thruster life and efforts are underway to model this behavior.

With the available data, failure of the Ir-coated Re material system was projected to occur by diffusion of the Re through the Ir, followed by subsequent oxidation and removal at the Ir surface. Thermogravimetric analysis [19] (TGA) was used to measure the oxidation rates of Ir and Ir–Re alloys. Rapid oxidation of specimens with 40 at.% Re was observed while little oxidation was observed at 20 at.% Re. This suggests imminent failure when the Re concentration at the surface exceeds 20 at.%. A life limit model [30] was then developed, as shown in Fig. 15. The life model, to date, has functional dependence on operating temperature, Ir-thickness and surface recession rate, but does not account for the possible favorable impact of the saturation of Re in Ir.

Other materials

Efforts are underway to provide materials with higher temperature, longer life capabilities than iridium-coated rhenium. One way is to develop enhanced protection [31] for Ir coated Re engines. A combi-

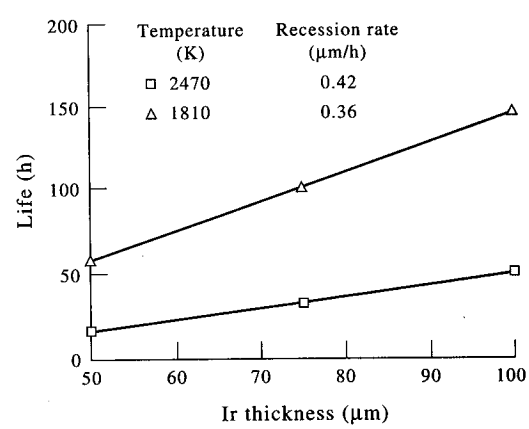

Fig. 15. Life prediction model for iridium-coated rhenium thrusters [30].

nation thermal/diffusive barrier using oxide coatings was chosen for development. The prime candidates are hafnia (HfO_2), zirconia (ZrO_2), and yttria (Y_2O_3). Another material system of high interest is mixed hafnium carbide (HfC) and tantalum carbide (TaC) ceramic composite reinforced with graphite fibers. HfC, TaC, and graphite are among the highest melting point materials known (4200, 4150, and 3800 K, respectively). These temperatures exceed the flame temperature of most propellants and could enable uncooled operation of hydrogen/oxygen rocket chambers. Mixed HfC/TaC coating on graphite fibers were successfully formed and oxidized [32] into protective oxide layers of HfO_2/Ta_2O_5. Some degree of stabilization of the HfO_2 was observed by the inclusion of the Ta_2O_5. The melting point of HfO_2 (3110 K) limits the operating temperatures in oxidizing environments. This temperature is well above the melting point of Ir, however, some cooling of rocket chambers fabricated with these materials may be required. Compositional variations of HfC/TaC are to be examined in order to determine that which provides the most adherent oxide coatings.

EARTH STORABLE ROCKET TECHNOLOGY

Small rocket chambers are usually radiation-cooled for simplicity. Radiation cooled operation, in general, required extensive fuel film cooling and its associated combustion/performance losses in order to reduce chamber material operating temperature and limit thermal soakback to the injector. Small rockets required larger percentages of their fuel for cooling than large rockets because of their larger surface-to-volume ratios and, therefore, stand to benefit the most from this high temperature material technology. Design of rockets requires a material property data base, including strength at elevated temperature, fatigue properties, and metallurgical joining techniques. Design for adequate fatigue strength during launch is a critical aspect of the design process.

Thruster design and fabrication with Ir-coated Re

The high operating temperature of Ir-coated Re (2500 K) allowed the elimination of fuel film cooling in Earth storable propellant rockets. In order to design and fabricate rockets using these materials, the materials property data base must be evaluated. Much of the basic work on measurement of properties was conducted in the 1960's and 1970's. This work was reviewed [19, 33], but sources are reported to have considerable variability. The method of fabrication and work hardening of the Re was a major uncertainty of critical interest. A comparison of the high temperature creep and tensile properties of rhenium fabricated by arc casting, CVD, and powder metallurgy was recently conducted [34]. The results of testing indicate that the creep-rupture properties of CVD rhenium are similar to those of powder metallurgy rhenium.

An investigation of metallurgical joining techniques of rhenium to dissimilar metals was also conducted [19]. Techniques such as inertia welding, furnace brazing, and electron beam (EB) welding were evaluated to join both wrought and CVD rhenium to Type 304L stainless steel, Hastelloy B2, and unalloyed niobium. Joints with titanium were not investigated. The inertia welding process successfully joined rhenium to niobium, however, joints with Type 304L stainless steel or Hastelloy B2 failed. Furnace brazing produced strong joints with all three materials investigated. Palcusil 25 and Nioro (BAU-4) braze filler metals were chosen based on their wetting ability on the four metals under investigation. The EB welding technique produced welds which were not true welds due to the great difference in melting temperature between rhenium and the other materials. These welds were more accurately described as a "parent metal braze". Ring shear specimens were then fabricated by these techniques and the fracture shear stress of these joints was obtained, showing that the practical joints are possible.

Thruster design issues which arose from the use of these high temperature materials included thermal management of the injector-chamber interface and design for adequate fatigue strength during launch. Thermal management can be accomplished by the use of fuel film coolant, mixture ratio control near the wall, or injector regenerative cooling. Design for adequate fatigue life is crucial and can be accomplished by the use of lighter weight materials, such as silicide coated niobium, for nozzle skirts where temperatures do not require rhenium and/or by providing adequate throat thickness. Requirements for throats up to a factor of 4 thicker than the chamber were predicted, depending on the rocket design. This increased thickness was predicted to raise the throat temperature less than 50 K and to be within the thermal limits of the material. An effort is underway to fabricate thick throat chamber designs to enable this design solution for adequate fatigue strength [35].

22 N rocket

Results from performance and life testing of a 22 N rocket design with N_2O_4/MMH propellants were reported first [19, 36]. The thruster was designed with a 150:1 area ratio nozzle for the direct comparison of performance of the Ir-coated Re engine with that of a flight qualified niobium engine of 690 kPa chamber pressure. Heat transfer to the injector due to soakback from the Ir-coated Re chamber was managed by using 30 to 40% fuel film cooling along with a patented staged combustion device to mix the film with the core flow further downstream such that the Ir-coated Re chamber ran essentially uncooled. This mixing of the film with the core flow resulted in a significant increase in combustion efficiency with no modification of the injector. As an added measure of design conservatism, a high emissivity dendritic rhenium surface was fabricated onto the outside of the

Table 2. 22 N iridium-coated rhenium rocket test summary at 150:1 area ratio [19]

MR	Maximum temperature (K)	Maximum specific impulse (s)	Duty cycle	No. of pulses	Duration (s)
1.59	2209	307	Steady	1	300
1.61	2156	304	Steady	1	5
1.62	2200	301	Steady	1	90
1.63	2229	310	Steady	1	350
1.64	2214	314	10%	2	95
1.64	1689	—	20%	1000	50
1.64	1700	—	40%	86,800	4340
1.64	1906	—	50%	1800	90
1.64	1972	—	60%	1400	70
1.64	2047	—	70%	2855	143
1.64	2094	—	80%	1706	85
1.64	2128	—	90%	2240	112
1.64	2153	—	Steady	2500	125
1.65	2237	311	Steady	1	90
1.66	2246	313	Steady	1	319
1.68	2259	318	Steady	2	110
Totals				100,311	6374

chamber to enhance radiation heat transfer from the chamber, especially during the shutdown transient. The measured vacuum specific impulse for this engine was 313 s at a mixture ratio of 1.66. This was nominally 20 s higher than that obtained with comparable niobium chambers. During these tests, the maximum wall temperatures were around 2200 K. The high emissivity external surface aided thermal management at the injector-chamber interface and reduced observed temperatures by about 250 K below those of the material demonstrator with little impact on performance. Duty cycle tests ranging from 10–90% on-time with each pulse being 0.050 seconds in duration were also conducted. Over 100,000 pulses were accumulated on the chamber. Based on temperature rise data, duty cycles of about 60–70% would have exceeded injector or valve temperature limits of 480 and 380 K, respectively. A rocket test summary of the 1.77 h of operation is given as a function of mixture ratio in Table 2. Inspection of the chamber after these tests revealed an Ir coating failure at the throat. This failure occurred at a sharp expansion in the flow (0.8 mm axial radius of curvature of the nozzle contour). For comparison, the successful material demonstrator chamber had a milder expansion with a 7.6 mm axial radius of curvature. Subsequent, postfire stress analyses indicated that the combination of small radius of curvature and high axial temperature gradient contributed to the coating failure.

A further series of tests was also conducted to determine thermal behavior with an expanded operating envelope of chamber pressure from 590 to 1100 kPa, 320 K propellants, and mixture ratios of 1.65 and 1.90. The more benign, low chamber pressure, low duty cycle tests were successfully completed, but other tests led to overheating of the injector/valves. Additional thermal design of this thruster is, therefore, required for this operating envelope.

Fabrication of larger thrusters requires a significant scale up of the CVD chamber fabrication technology and low deposition rates for the iridium coating initially resulted in local blistering of the coating. A metallurgical investigation of the coating revealed contamination sandwiched between the multiple layers of iridium in the 50 μm thick coating. A program was then undertaken to improve the CVD iridium deposition process [35]. The deposition rate was improved by taking advantage of natural convection flows within the CVD chamber to deliver more precursor material to the surface of the mandrel. In addition, a fluidized bed evaporator was developed to enable a continuous feed of evaporated iridium precursor material. Continuous iridium deposition at about 15 μm/h then enabled the elimination of the previously experienced contamination in the scaled up CVD process by depositing the coating in one continuous deposition run.

62 N rocket

This improved CVD fabrication technology was first demonstrated on a 62 N chamber with N_2O_4/MMH propellants of 690 kPa and a 75:1 area ratio [20, 37, 38]. This chamber was chosen to demonstrate that iridium-coated rhenium chambers could be retrofitted on existing Nb rockets without modification of the injector. Soakback heat transfer to the injector was managed by the fuel film cooling along with a patented staged combustion device to mix the film with the core flow such that the Ir-coated Re chamber runs essentially uncooled. This mixing of the film with the core flow resulted in a significant performance increase with no modification of the injector. As an added measure of design conservation, a high emissivity dendritic rhenium surface was fabricated onto the outside of the chamber to enhance radiation heat transfer from the chamber, especially during the shutdown transient. A total firing time of 600 s and 263 cycles were accumulated

Table 3. 62 N iridium-coated rhenium rocket test summary at 75:1 area ratio [20]

MR	Maximum temperature (K)	Maximum vacuum specific impulse (s)	Duty cycle	No. of pulses	Duration (s)
1.41	—	300	Steady	1	20
1.54	2056	300	Steady	1	15
1.54	—	—	10%	80	8
1.57	2116	306	Steady	3	41
1.59	2113	303	Steady	2	25
1.60	2117	305	Steady	1	20
1.62	—	—	Steady	1	5
1.63	2128	301	Steady	2	15
1.63	2194	—	10%	80	8
1.64	2186	306	Steady	7	280
1.64	—	—	10%	80	8
1.65	2155	305	Steady	1	10
1.66	2182	305	Steady	2	115
1.68	2159	305	Steady	1	10
1.82	—	303	Steady	1	20
Totals				263	600

Table 4. 440 N iridium-coated rhenium rocket test summary at 22:1 area ratio [39]

MR	Maximum temperature (K)	Maximum vacuum specific impulse (s)	No. of cycles	Duration (s)
1.54	—	290	1	15
1.60	—	289	3	609
1.62	2100	292	3	1927
1.63	2123	291	2	1310
1.64	2094	292	4	2950
1.65	2222	292	8	4102
1.66	2169	293	5	3000
1.67	2144	293	6	1052
1.69	2144	294	1	35
Totals			33	15,000

on one of the chambers with no degradation. A test summary is given in Table 3. Chamber temperatures ranged from 2050 to 2150 K, indicating that the high emissivity chamber surface was not required. Measured specific impulse was 305 s at a mixture ratio of 1.65. This compares to 286 s specific impulse obtained with a flight qualified Nb design. Thruster performance was successfully demonstrated over the flight qualification inlet pressure, mixture ratio operating envelope. When comparing the Re chamber with a Nb chamber, post test chamber discoloration streaks suggested more complete combustion and less plume contamination with the Re chamber. The final hurdle for this chamber was an acceptance test to determine whether the material and design had the requisite fatigue properties to survive the launch vibration environment. This test was successfully passed although analyses indicated the design was marginal. Increasing the material thickness at the throat can alleviate this concern and a demonstration of this fabrication technology is underway [35].

440 N rocket

Following the successful material demonstration [19, 24], the Jet Propulsion Laboratory undertook to demonstrate a 440 N thruster [39, 40] on N_2O_4/MMH propellants at a nominal chamber pressure of 690 kPa. Fuel regenerative cooling of the injector was employed to manage the soakback heat transfer and no high emissivity dendritic surface was employed. A total firing time of 4.2 h and 33 cycles were accumulated on one of the chambers with temperatures ranging from 2100 to 2200 K. A performance of 292 s was measured at a mixture ratio of 1.65 and an area ratio of 22:1. This performance was about a 10 s higher than a similar Nb engine, showing the decreased benefit of high temperature materials as thrust class increases. A summary of these tests is given in Table 4 as a function of mixture ratio.

The improved CVD fabrication technology was demonstrated on a 440 N thruster. Performance and durability tests are underway on this engine with N_2O_4/MMH propellants [20, 41]. Performance achieved on the JPL program [39, 40] was duplicated

Table 5. 440 N iridium-coated rhenium rocket test summary at 47:1 area ratio [20]

MR	Maximum temperature (K)	Maximum vacuum specific impulse (s)	No. of cycles	Duration (s)
1.43	—	—	1	5
1.49	2167	—	2	442
1.50	—	—	3	37
1.51	—	—	1	514
1.58	—	300	2	30
1.59	2151	302	2	1217
1.60	2223	303	2	710
1.61	2146	—	7	1452
1.62	2162	300	4	1046
1.63	2153	—	1	503
1.64	2253	303	4	1133
1.65	2192	301	4	1939
1.66	2203	301	8	2534
1.67	2064	301	2	597
1.70	—	—	4	52
1.80	2227	303	1	600
1.86	—	—	2	40
1.90	—	—	2	15
Totals			52	12320

at an area ratio of 22:1. A total of 3.4 h test time and 52 thermal cycles were accumulated on this engine at the 47:1 area ratio. A summary of these tests is given in Table 5. Also, performance data was obtained on a high area ratio (286:1) flight type engine. Evaluation of the data indicated a nominal vacuum specific impulse of 322 s, at a mixture ratio of 1.65. A summary of these tests is given in Table 6, giving a cumulative total of 3.7 h and 72 thermal cycles on a single chamber when added to the 47:1 area ratio tests. An effort is underway to evaluate this thruster over envelopes typical of apogee rocket qualifications. Analyses indicate, however, that significantly thicker throats are required to survive the launch vibration environment.

550 N rocket

Preliminary test results from a second thruster manufacturer with a 550 N chamber on N_2O_4/N_2H_4 propellants were obtained [42]. Vacuum specific

Table 6. 440 N iridium-coated rhenium rocket test summary at 286:1 area ratio [20]

MR	Maximum temperature (K)	Maximum vacuum specific impulse (s)	No. of cycles	Duration (s)
1.46	1991	318	1	25
1.51	2017	319	1	120
1.58	2066	321	1	100
1.59	2068	322	4	195
1.60	1941	321	1	10
1.61	2139	321	1	120
1.62	2134	321	2	33
1.64	2082	323	3	155
1.65	—	322	2	30
1.67	2033	322	2	121
1.79	2132	322	1	25
1.00	2139	322	1	52
Totals			20	986

impulses in the 326–328 s range were estimated at an area ratio of 204:1. A combustion (c-star) efficiency in excess of 98% theoretical was achieved with rhenium chamber temperatures below 1900 K. Further injector optimization is projected to yield a specific impulse of 330 s.

High pressure rocket technology

The Earth storable liquid rocket technology currently available for NASA and commercial spacecraft uses relatively low system pressures in comparison to that of recent DOD programs [43]. The performance of low pressure rocket nozzles is known to be adversely affected by frozen flow losses on the order of 10–20 s of specific impulse. There is promise that these losses can be significantly reduced by operation at higher chamber pressures. In addition, there may be a favorable impact on rocket combustion chamber efficiency with increased chamber pressure. Dry weight penalties associated with pressure-fed propulsion systems operated at high pressure, however, have usually offset any performance improvement. Recent developments in advanced propellant tankage and in miniaturizing subsystem components for small satellites may have altered this system optimization. High temperature materials may offer the thermal margin necessary to withstand the increased heat fluxes associated with high pressure rocket chambers, without paying a performance penalty for film cooling. Finally, operation at high pressure allows the reduction in size of rockets. Rocket size reduction can potentially be used, along with the miniaturization of propulsion system components to greatly benefit a growing small satellite industry. A technology program is currently planned.

HIGHER PERFORMANCE PROPELLANTS

Higher performance on-orbit propulsion systems can be obtained by developing the technology for more energetic propellants. System considerations were analyzed to indicate new propellant combinations of interest to low thrust chemical rockets. Maximum potential for mission usage was expected for geosynchronous satellites for communication, surveillance, tracking, earth observation, and meteorological functions. Manned spacecraft have different criteria and systems considerations with high leverage to be derived from the integration of propulsion, power, and life support systems. There are very different criteria and systems considerations for optimizing propulsion systems of different mission classes. Optimizations can be performed on performance, density impulse, contamination, and toxicity. The ability to be integrated with other systems, storability, and cost may also be important system considerations. Low thrust propulsion systems, in general, are required to provide frequent and rapid restarts, high cyclic life, and the flexibility to operate over a wide range of environmental conditions, often with long quiescent periods.

Space storable propellants

An evolutionary growth path to more energetic propellants is proposed with a new class of propellants defined as "space storables", which provide a link between upgraded "Earth storables" and cryogenic systems. "Space storables" are defined as those propellants that can be passively stored, within mission constraints, without active cooling or refrigeration. Recent developments in cryogenic storage technology have placed liquid oxygen (LOX) in this category and it was selected as the first space storable oxidizer for evaluation because it is readily available and has validated handling procedures. Another candidate may be ClF_5 with several fuel candidates. Liquid hydrogen, at this time, is not considered space storable due to its low storage temperature, however, it is a candidate fuel for manned spacecraft due to potential systems benefits from integration with life support systems. Nitrogen hydrides and hydrocarbons are considered the chief space storable fuels and there are justifications for the selection of fuels from each of these categories. Hydrazine was selected as the fuel for spacecraft with sensors which are sensitive to carbon containing compounds. The Space Storable Rocket Technology Program [44] also provided justification for the selection of hydrazine as the fuel based on the "dual mode" propulsion systems for geosynchronous satellites. In these systems, common tankage for the apogee and stationkeeping propulsion provides the major system level benefit. An 880 N thrust, 1380 kPa chamber pressure rocket technology program is underway utilizing the pintle injector. Eight pintle configurations were evaluated indicating performances up to 95% theoretical c-star, which yielded a vacuum specific impulse of 345 seconds at an area ratio of 204:1. The application of high temperature materials is currently under evaluation for this program.

A facility modification is currently underway at LeRC to develop technology for the propellant combinations LOX/ethanol and LOX/methane. These propellants are considered as candidates for auxiliary propulsion systems on launch vehicles [45] where their nontoxic, noncorrosive properties promise reductions in operational costs for reusable spacecraft.

Integrated hydrogen/oxygen propellants

Hydrogen/oxygen (H/O) auxiliary propulsion technology for integrated propulsion systems requires that specific thrusters be developed. The technology base for this development exists from the Space Shuttle technology programs [46] of the late 1960's. Technology for both gaseous and liquid thrusters was demonstrated and was used recently to demonstrate 110 N gaseous thrusters under the Space Station Freedom propulsion technology program [47]. A systems analysis [46] of a proposed liquid hydrogen/

liquid oxygen primary Reaction Control System (RCS) and a gaseous hydrogen/gaseous oxygen vernier RCS indicated a significant payload benefit for integrated H/O systems on launch vehicles and this was substantiated [48] using detailed mass properties from the Space Shuttle Orbiter. Further analysis [49] of this integrated H/O concept, however, revealed several abort scenarios that were problematic for the proposed system and, alternatively, proposed both primary and vernier gaseous H/O systems based on the lowest life cycle costs, which included the cost of development, production, and operation of the propulsion system. The liquid H/O RCS system in the study [49] had the lowest system weight, but was heavily burdened with development costs. A review [50] of this program and prior H/O technology indicted that further maturation of this technology was required, but that the technology base was demonstrated.

SUMMARY

A broad technology program to improve the performance of low thrust chemical rockets was reviewed. Navier–Stokes analyses of low Reynolds number rocket flows were compared with local flow property measurements obtained via Rayleigh and Raman diagnostics in a 110 N gaseous hydrogen/gaseous oxygen rocket. Performance trends with mixture ratio and fuel film cooling were predicted, but were 3–4% below measured performance values. This indicated that the computational domain should include the near injector flow and that the shear layer combustion model needed improvement. In another effort, a spray combustion model was assembled for liquid rockets and is undergoing evaluation.

Recommended life limtis of silicide-coated Nb thrust chambers used by several manufacturers of state-of-the-art thrusters were given as a function of operating temperature and duty cycle. Significant variability in recommended life was noted along with a general agreement that there was about 10–15 h of life at 1640 K. For cyclic applications, a limit of between 100 and 1000 thermal cycles was indicated, depending on operating temperature. A materials technology program to fabricate and substitute iridium-coated rhenium thrust chambers was reviewed. These new materials enabled the fabrication of radiation cooled thrust chambers with significant performance increases due to the mixing of the film coolant with the core flow by a patented staged combustion device which essentially eliminates fuel film cooling. Over fifteen hours of operation and 2684 cycles at operating temperatures of 2500 K was demonstrated on these materials without failure with N_2H_4/MMH propellants. The life limiting process in iridium-coated rhenium material was evaluated from fundamental measurements. The process of failure was described as the diffusion of rhenium through the iridium coating until an alloy composition in excess of 20% Re occurs on the surface which then can result in catastrophic material loss to oxidation.

The design and fabrication of rockets using iridium-coated rhenium materials was outlined and the results of four different rocket test programs with these materials was reviewed. Rockets in the thrust classes of 22, 62, 440, and 550 N were tested by two different contractors with excellent results. Performance of iridium-coated rhenium rockets was nominally 20 s higher than comparable niobium rockets in the 22 N class and nominally 10 s higher in the 440 N class. Design and fabrication of chambers to survive the launch vibration environment is underway.

An evolutionary path to more energetic propellants is being followed with the development of "space storable" propellants defined to include liquid oxygen (LOX) as the oxidizer and nitrogen hydrides or hydrocarbons as the fuel. Tests with a LOX/N_2H_4 rocket indicated that 95% theoretical c-star performance was possible, for a vacuum specific impulse of 345 s at an area ratio of 204:1. In another effort, an in-house facility modification is underway to test up to 440 N rockets with LOX/CH_4 or LOX/C_2H_5OH. Finally, technology reviews and systems analyses of integrated H/O systems for manned spacecraft were conducted. Gaseous H/O systems provided the lowest life cycle costs for launch vehicles at this time. However, liquid H/O systems had the lowest weight. The technology base for low thrust H/O rockets exists, but flight systems require that specific thrusters be developed.

REFERENCES

1. G. R. Nickerson, D. E. Coats, A. L. Dang, S. S. Dunn and H. Kehtarnavaz, Two-dimensional kinetics (TDK) nozzle performance computer program. NASA CR-890124 (1989).
2. G. P. Richter and H. G. Price, Proven, long-life hydrogen/oxygen thrust chambers for space station propulsion, NASA TM-88822, *JANNAF Propulsion Meeting*, New Orleans (1986).
3. S. C. Kim and T. J. VanOverbeke, Performance and flow calculations for a gaseous H_2/O_2 thruster. *J. Spacecraft Rockets* **28,** (1991).
4. J. M. Weiss and C. L. Merkle, Numerical investigation of reacting flowfields in low-thrust rocket engine combustors. AIAA-2080 (1991).
5. J. M. Weiss, R. L. Daines and C. L. Merkle, Computation of reacting flowfields in low thrust rocket engines. AIAA 91–3557 (1991).
6. J. S. Shuen and S. Yoon, Numerical study of chemically reacting flows using a lower-upper symmetric successive overrelaxation scheme. *AIAA J.* **27,** 1752–1760 (1989).
7. S. C. Kim, Numerical study of high-area-ratio H_2/O_2 rocket nozzles. AIAA 91–2434 (1991).
8. B. D. Reed, P. F. Penko, S. J. Schneider and S. C. Kim, Experimental and analytic comparison of flowfields in a 110 N (25 lbf) H_2/O_2 rocket. AIAA 91–2283 (1991).
9. L. A. Arrington and B. D. Reed, Comparison of Axisymmetric and three-dimensional hydrogen film coolant injection in a 110 N hydrogen/oxygen rocket. AIAA 92–3390 (1992).
10. L. A. Arrington and S. J. Schneider, Low thrust rocket test facility. AIAA 90–2503 (1990).

11. R. G. Seasholtz, F. J. Zupanc and S. J. Schneider, Spectrally resolved Rayleigh scattering diagnostic for hydrogen-oxygen rocket plume studies. AIAA 91–0462 (1991).
12. F. J. Zupanc and J. M. Weiss, Rocket plume flowfield characterization using laser Rayleigh scattering. AIAA 92–3351 (1992).
13. S. M. Dash, H. S. Pergament, D. E. Wolf, N. Sinha, M. W. Taylor and M. E. Vaughn Jr, JANNAF Standardized Plume Flowfield Code Version II (SPF-II), CR-RD-SS-90-4 (1990).
14. W. A. DeGroot, The development of a fiber optic raman temperature measurement system for rocket flows. AIAA Paper 91–2316 (1991).
15. W. A. DeGroot and J. M. Weiss, Species and temperature measurement in H_2/O_2 rocket flow fields by means of Raman scattering diagnostics. AIAA Paper 92-3353 (1992).
16. L. Larosiliere, R. Litchford and S. M. Jeng, Hypergolic bipropellant spray combustion and flow modelling in rocket engines. AIAA Paper 90–2238 (1990).
17. A. A. Amsden *et al.*, KIVA-II: a computer program for chemically reactive flows with spray. Los Alamos National Laboratory Report LA-11560-MS (1989).
18. L. M. Larosiliere and S. M. Jeng, Bipropellant spray combustion modeling in small rocket engines. AIAA 91–2197 (1991).
19. J. R. Wooten and P. T. Lansaw, High-temperature oxidation-resistant thruster research. NASA CR-185233 (1990).
20. Advanced small rocket chambers, NASA Contract NAS3-25646. Final report. To be published.
21. J. T. Harding, R. H. Tuffias and R. B. Kaplan, Platinum group coatings for refractory metals. AFRPL-TR-84-035 (1984).
22. J. T. Harding, R. H. Tuffias, R. B. Kaplan and K. Chandler, Oxidation resistant coatings for refractory metals. JANNAF Propulsion Meeting, (1985).
23. J. T. Harding, J. M. Kazaroff and M. A. Appel, Iridium-coated rhenium thrusters by CVD. *Second Int. Conf. on Surface Modification Technologies*, Chicago, Ill., September (1988).
24. M. V. Whalen, P. T. Lansaw and J. R. Wooten, High-temperature oxidation-resistant thrusters. 1987 *JANNAF Propulsion Meeting*, San Diego, Calif. (1987).
25. S. D. Rosenberg, D. M. Jassowski, R. Barlow, R. Lucht, K. McCarty and R. Stulen, Combustion interaction with radiation-cooled chambers. AIAA 90–2121 (1990).
26. R. S. Barlow, R. P. Lucht, D. M. Jassowski and S. D. Rosenberg, Gas-phase measurements of combustion interaction with materials for radiation-cooled chamber. AIAA 91–2216 (1991).
27. R. H. Stulen, D. R. Boehme, W. M. Clift and K. F. McCarty, Characterization of Iridium Coated Rhenium used in high-temperature, radiation-cooled rocket thrusters. *JANNAF Propulsion Meeting*, Anaheim, Calif. (1990).
28. J. C. Hamilton, N. Y. C. Yang, W. M. Clift, D. R. Boehme, K. F. McCarty and J. E. Franklin, Diffusion mechanisms in chemical vapor-deposited iridium coated on chemical vapor-deposited rhenium. *Metall. Trans.* **23A,** p. 851 (1992).
29. D. A. Outka, J. C. Hamilton, W. M. Clift, N. Y. C. Yang and D. R. Boehme, High temperature diffusion in CVD iridium coatings on CVD rhenium. 182*nd Annual Meet. of Electrochem. Soc.* (1992).
30. S. J. Schneider, High-temperature thruster technology for spacecraft propulsion. IAF Paper 91–254, 42*nd Congr. Int. Astronaut. Fedn*,. Montreal, Canada (1991).
31. R. H. Tuffias, G. J. Melden and J. T. Harding, Enhanced oxidation protection for iridium-lined rhenium thrust chambers. NASA Contract NAS3-25648, Final Report ULT/TR-90-7234 (1990).
32. H. O. Pierson, J. G. Sheek and R. H. Tuffias, Overcoating of carbon–carbon composites. WRDC-TR-89-4045 (1989).
33. B. D. Bryskin, Evaluation of properties and special features for high-temperature applications of rhenium. *Ninth Symp. Space Nuclear Power Systems*, Albuquerque, N.M. (1992).
34. R. C. Svedberg and W. W. Bowen, High temperature creep and tensile properties of chemically vapor-deposited rhenium. D.O.E. Report No. HEDL-SA-2695-FD, *Metall. Coatings and Process Tech. Conf.*, San Diego, Calif., April (1982).
35. R. H. Tuffias, G. J. Melden and J. T. Harding, CVD iridium process control and improvement and chamber fabrication. NASA Contract NAS 3-25792. Final Report. To be published.
36. J. R. Wooten and P. T. Lansaw, The enabling technology for long-life, high performance on-orbit and orbit-transfer propulsion systems: high-temperature oxidation resistant thrust chambers. *JANNAF Propulsion Meeting*, Cleveland, Ohio (1989).
37. S. Rosenberg and L. Schoenman, A new generation of high performance engines for spacecraft propulsion. AIAA 91–2039 (1991).
38. S. D. Rosenberg and L. Schoenman, High performance bipropellant engines for orbit transfer and attitude control propulsion. IAF Paper 91–249, 42*nd Congr. Int. Astronaut Fedn*, Montreal, Canada (1991).
39. L. Schoenman, J. Franklin and P. T. Lansaw, Feasibility demonstration of a high-performance 100 lbf rocket engine. Jet Propulsion Laboratory Contract 957882. Final Report (1989).
40. M. A. Appel, L. Schoenman, J. E. Franklin and P. T. Lansaw, Feasibility demonstration of a 445 N high-performance rocket engine. *JANNAF Propulsion Meeting*, Cleveland, Ohio (1989).
41. S. D. Rosenberg, L. Schoenman and D. M. Jassowski, High performance storable bipropellant orbit transfer engine. IAF Paper 92–0672, 43*rd Congr. Int. Astronaut. Fedn*, Washington, D.C. (1992).
42. Personal communication with R. Sackheim of TRW Space and Technology Group.
43. J. R. Stuart and J. Gleave, Key Small Satellite Subsystem Developments AIAA 90–3576, (1990).
44. M. L. Chazen, T. Mueller, A. R. Casillos and D. Huang, Space storable rocket technology program. Final Report-Basic Program, NASA CR-189131 (1992).
45. G. F. Orton and T. D. Mark, LOX/hydrocarbon auxiliary propulsion for the space shuttle orbiter. *J. Spacecraft* **21,** 580–586 (1984).
46. S. J. Schneider, Auxiliary propulsion technology for advanced earth-to-orbit vehicles. NASA TM-100237 *JANNAF Propulsion Conf.* San Diego, Calif. (1987).
47. R. E. Jones, P. R. Meng, S. J. Schneider, J. S. Sovey and R. R. Tacina, Space station propulsion system technology. NASA TM-100108, 38*th Int. Astronaut. Fed. Congr. Brighton* (1987),
48. *S. J. Schneider and B. D. Reed, Weight savings in aerospace vehicles through propellant scavenging. NASA TM*-100900 *or Weight Engng* **48,** 11–25 (1989).
49. D. L. Gerhardt, Integrated hydrogen/oxygen technology applied to auxiliary propulsion systems—final report. NASA CR-185289 (1990).
50. B. D. Reed and S. J. Schneider, Hydrogen/oxygen auxiliary propulsion technology. NASA TM-105249 or AIAA 91–3440, *Conference on Advanced Space Exploration Initiatives Technologies*, Cleveland, Ohio (1991).